13th IEA Heat Pump Conference
April 26-29, 2021 Jeju, Korea

Numerical simuation of two-phase flow distribution in a vertically installed refrigerant distributor

Siyoung Choi[a], Hyoin Lee[a], Jihwan Jeong[a]*

[a] School of Mechanical Engineering, Pusan Nat'l Univ, 2, Busandaehak-ro 63beon-gil, Geumjeong-gu, Busan, 46241, Republic of Korea

Abstract

If two-phase flow occurs in the Variable Refrigerant Flow (VRF) system air conditioner, the distribution characteristic may be changed, and uneven distribution problem will occur. In addition, changing the orientation of the refrigerant distributor from horizontal to vertical in order to reduce the installation space, this uneven distribution becomes even worse. In this study, computational fluid dynamics (CFD) simulation is used to calculate uneven distribution of two-phase flow in a vertically installed distributor and to analyze the factors affecting the uneven distribution by analyzing the internal flow. CFD results are validated by the previous experimental results. Due to the momentum difference, liquid phase flows toward the end of the header and the gas phase flows near the inlet. Uneven distribution is exacerbated as the void fraction increased. The geometry of the header is modified to improve the non-uniform distribution and the result are compared with the existing data.

Selection and/or peer-review under responsibility of the organizers of the 13th IEA Heat Pump Conference 2020.

Keywords: computational fluid dynamics (CFD), distribution, two-phase

1. Introduction

Variable Refrigerant Flow (VRF) system is an air conditioning system that supplies refrigerant to several indoor units using one outdoor unit. VRF system has high efficiency because it can control the cooling and heating depending on thermal loads of each indoor space. Due to its convenience and efficiency, demand is increasing in commercial and residential buildings. VRF system supplies the refrigerant to each indoor unit by using a refrigerant distributor, and the refrigerant distributor can also be connected to other refrigerant distributors. As the height of a building increases, the height difference criteria of the refrigerant distributor also increase. In a vertical pipe connecting the distributor, the refrigerant flowing in the liquid state can be vaporized into a two-phase state due to the static pressure loss caused by the height difference. When a two-phase flow is supplied to the refrigerant distributor, unlike the distribution tendency of a single phase flow, uneven distribution occurs. In addition, in order to reduce the installation space, there is a demand to change the direction of the refrigerant distributor from horizontal to vertical. If the refrigerant is distributed to each indoor unit through a vertically installed distributor, the uneven distribution can be worse than the horizontal installation. If uneven distribution occurs inside the refrigerant distributor for the influence of such supply conditions, some of the indoor units do not receive sufficient refrigerant mass flow rates to meet their thermal demand. Then, the outdoor unit will have additional operation to supply the required mass flow rate in the indoor space, and it will be a negative impact on the energy efficiency of the system. Therefore, it is necessary to investigate the distribution characteristics when the two-phase flow is supplied to the vertically installed refrigerant distributor.

The refrigerant distributor is a manifold shape. The flow distribution problem in the manifold shape has been mainly dealt with in the research of parallel-flow heat exchangers. Many researchers [1-6] have conducted experimental and numerical studies on the flow distribution in parallel-flow heat exchangers. Dario et al. [1] reviewed the study of two-phase flow distribution in parallel channels and summarized the factors that influence the two-phase flow distribution. The factors affecting the distribution are divided into geometrical

factors, fluid properties, and operating conditions. Kim et al. [2] experimentally investigated the two-phase flow distribution of R-134a in a downward flow mini-channel heat exchanger varying the operating conditions (mass flux, quality), geometrical factor (inlet position) and compared with the data conducted with R-410A. Vist and Pettersen [3] experimentally investigated the two-phase distribution varying geometrical factors (header diameter, flow direction) and operating conditions (mass flow rate, quality, heat load). Lee and Lee [4] experimentally investigated the two-phase distribution tendency varying the geometrical factor (intrusion depth) and operating conditions (mass flux, quality). Zhou et al. [5] numerically investigated the flow distribution in a central-type parallel heat exchanger. Flow distribution by changing the geometrical factor (dividing and combining header ratio, header and tube diameter ratio) was mainly considered. Said et al. [6] numerically investigated reducing mal-distribution at heat exchanger by installing orifice and nozzle between header and branch tubes.

In the previous study, many researchers conducted experimental and numerical study on flow distribution in heat exchangers. As a result, geometric factors and flow conditions affected the flow distribution in the manifold. In the case of experimental study, however, there are limitations in the analysis of the internal flow characteristic of header by installing the measurement device inside the distributor. In the numerical study, the flow characteristic in the header by the change of geometrical factor was performed by 3-D simulation, but the analysis was mainly dealt with in single phase flow.

In this study, computational fluid dynamics (CFD) simulation is conducted to investigate the two-phase flow distribution characteristics in a vertically installed distributor used in the VRF system. The distributor shape is modeled by simulating the refrigerant distributor used in the VRF system, and the two-phase flow distribution is calculated by changing the inlet tube position and void fraction. Two-phase flow inside the header are analyzed through quantitative values such as the void fraction of the cross-section and the superficial velocity. Based on the analysis, the geometry of the distributor is modified to improve the flow distribution. Then distribution characteristics of the modified distributor are compared with those of the existing distributor.

2. Numerical Method

2.1. Geometry

The VRF system consists of three pipes, two of them are gas pipe and the other is a liquid pipe. The two-phase flow due to height difference occur in the liquid pipe of refrigerant distributor. The modelling of refrigerant distributor is shown in Fig. 1. The header is installed vertically, and the shape of the header is a double pipe through which a circular tube passes in the center. Then four circular branch tubes for supplying the refrigerant to each indoor unit are installed having the 3mm of intrusion depth. The number of each branch tube is named from channel #1 to channel #4 according to the installed location from the top to the bottom. The direction of inlet tube is horizontal and is perpendicular to the installation direction of the branch tube. The position of the inlet tube varies depending on the analysis conditions.

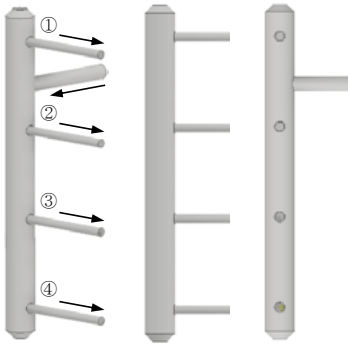

Fig. 1. Modelling of Refrigerant Distributor

2.2. Governing Equation

Transient analysis is conducted to calculate two-phase flow distribution in the distributor modelled in chapter 2.1. The commercial CFD code STAR-CCM+ is used for the numerical computations. A second order upwind scheme is used to discretize the velocity convective term and SIMPLE (Semi-Implicit Method for Pressure-Linked Equations) algorithm is adopted for the velocity-pressure coupling in STAR-CCM+

The flow pattern of two-phase flow inside the header was bubbly flow [7]. Therefore, Eulerian-Eulerian model is adopted to solve the governing equation. In Eulerian-Eulerian approach, each phase is treated mathematically inter-penetrating continua and mixed in each control volume. Then, governing equations are solved for each phase. Assuming adiabatic and incompressible flow, continuity and momentum equation of each phase is given as follows:

$$\frac{\partial}{\partial t}(\rho_k \alpha_k) + \frac{\partial}{\partial x_i}(\rho_k \alpha_k U_{i,k}) = 0 \tag{1}$$

$$\frac{\partial}{\partial t}(\rho_k \alpha_k U_{i,k}) + \frac{\partial}{\partial x_j}(\rho_k \alpha_k U_{i,k} U_{j,k}) = -\alpha_k \frac{\partial p}{\partial x_i} + \alpha_k \rho_k g_i + \frac{\partial}{\partial x_j} \mu \alpha_k \left[\left(\frac{\partial U_j}{\partial x_i} + \frac{\partial U_i}{\partial x_j} \right) - \frac{2}{3} \frac{\partial U_j}{\partial x_j} \delta_{ij} \right] + M_{i,k} \tag{2}$$

where α_k and $M_{i,k}$ represent the volume fraction of phase k and interfacial momentum transfer. In this study, Inlet tube, manifold, branch tubes have different flow directions each other. To model the momentum transfer of interface, dispersed phases are assumed spherical particle and only the drag force is considered in this study. Drag is interfacial force that disturbs the flow of bubbles by the surrounding liquid. For drag coefficient C_D, Schiller and Naumann drag coefficient [8] is chosen. Drag force and drag coefficient are given as follows:

$$F_d = \frac{3}{4} \frac{C_D}{d_b} \alpha \rho_c |U_r| U_r \tag{3}$$

$$C_D = \begin{cases} \frac{24}{Re_d}\left(1 + 0.15 Re_d^{0.687}\right) & 0 < Re_D \le 1000 \\ 0.44 & Re_D > 1000 \end{cases} \tag{4}$$

Where Re_d and ρ_c represent the Reynolds number of dispersed phase and density of continuous phase. To calculate turbulence, RANS model is used, which is calculated by dividing the average component and the variation component. Since the Eulerian-Eulerian model is used, the turbulence model of each phase is also calculated separately. In the case of continuous phase, the Realizable K-epsilon model is used, which modify the standard k-e model to calculate the Reynolds stress [9]. The equations for turbulence kinetic energy k and turbulence dissipation rate ε are as follows:

$$\frac{\partial \alpha_c \mathrm{k_c}}{\partial \mathrm{t}} + \frac{\partial (\alpha_c \mathrm{k_c} U_{i,c})}{\partial x_j} = \frac{1}{\rho_c} \frac{\partial}{\partial x_j} \left[\alpha_c \left(\mu_c + \frac{\mu_{T,c}}{\sigma_k} \right) \frac{\partial \mathrm{k_c}}{\partial x_j} \right] + \alpha_c \frac{\mu_{T,c}}{\rho_c} \left(\frac{\partial \mathrm{U_{i,c}}}{\partial \mathrm{x_j}} + \frac{\partial \mathrm{U_{j,c}}}{\partial \mathrm{x_i}} \right) \frac{\partial \mathrm{U_{i,c}}}{\partial \mathrm{x_j}} - \alpha_c \varepsilon_c \tag{5}$$

$$\frac{\partial \alpha_c \varepsilon_c}{\partial \mathrm{t}} + \frac{\partial (\alpha_c \varepsilon_c U_{i,c})}{\partial x_j} = \frac{1}{\rho_c} \frac{\partial}{\partial x_i} \left[\alpha_c \left(\mu_c + \frac{\mu_{T,c}}{\sigma_\varepsilon} \right) \frac{\partial \varepsilon_c}{\partial x_j} \right] + \alpha_c C_1 \frac{\varepsilon_c}{2} \left(\frac{\partial \mathrm{U_{i,c}}}{\partial \mathrm{x_j}} + \frac{\partial \mathrm{U_{j,c}}}{\partial \mathrm{x_i}} \right) \frac{\partial \mathrm{U_{i,c}}}{\partial \mathrm{x_j}} - \alpha_c C_2 \frac{\varepsilon_c^2}{k_c + \sqrt{(\mu_c/\rho_c)\varepsilon_c}} \tag{6}$$

where α_c represents volume fraction of continuous phase.

Turbulence response model is used to calculate the turbulence of the dispersed phase. The turbulence of dispersed phase is correlated from the turbulence of the continuous phase by using the correlation derived from the response coefficient. In this study, the Issa response coefficient which is a function of void fraction is used [10].

2.3. Grid

To generate the mesh in fluid domain, polyhedral mesh and prism layer mesh are applied. In order to calculate the turbulence, the area identified by the law of wall should be generated in a compact grid and calculated for each area. In this study, the prism layer thickness is generated to satisfy $y^+ < 5$ condition to calculate the turbulence from the viscous sublayer. To determine the base size of polyhedral mesh, grid

independence test is performed by comparing the y-axis velocity distribution in the branch tube and the base size is determined to be 8,200,000 cells.

2.4. Boundary Condition

The working fluid in this study is an air-water mixture. The void fraction is calculated by assuming a slip ratio of 1 when the quality of the refrigerant is varied from 0 to 0.1. The mass flow rate of air and water are determined by using the same void fraction. The wall is assumed an adiabatic wall and no-slip condition. Inlet boundary condition is set to mass flow boundary condition. The mass flow rate of water is $0.26\ \mathrm{kg/s}$, and the mass flow rate of air is varied in the range of $1.16 \times 10^{-4} \sim 9.70 \times 10^{-4}\ \mathrm{kg/s}$ depending on the void fraction. The outlet boundary condition is selected as the pressure boundary condition and set to 0 Pa based on the atmospheric pressure. The inlet boundary conditions used in the analysis are shown in Table 1.

Table 1. Inlet boundary condition of air and water

Material	Volume flow rate [kg/s]
Water	0.26
Air at $\alpha = 0.17$	1.16×10^{-4}
Air at $\alpha = 0.39$	4.43×10^{-4}
Air at $\alpha = 0.53$	9.70×10^{-4}

3. RESULT AND DISCUSSION

3.1. Simulation Results and Validation

CFD simulation is used to calculate the two-phase flow distribution in the header according to the inlet position and the void fraction change. The void fraction has been changed from 0.17 to 0.53 and the inlet position is located at the top or bottom of the header and is called the upper inlet and bottom inlet in each case. The calculated mass flow results show fluctuations, and time-averaged values are used. The mass flow rate distributed to each branch tube is represented by Liquid Fraction which is the ratio of the mass flow rate distributed to each branch tube to the total mass flow rate. The distribution tendency calculated by CFD are compared with the experimental data conducted by Ham [7]. A comparison of results is shown in Fig. 2.

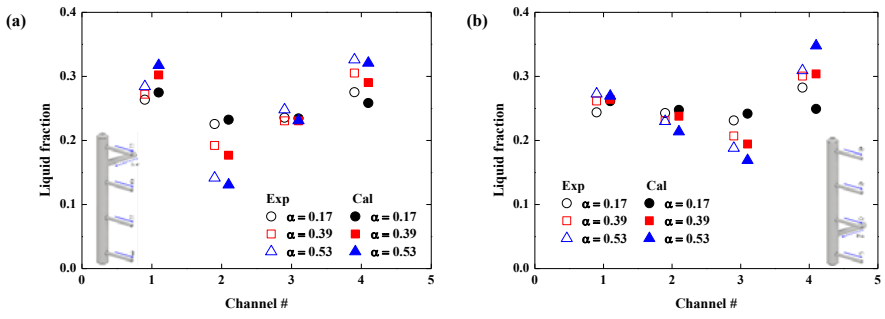

Fig. 2. Validation with The Experimental Data by Ham[7]: (a) Upper Inlet, (b) Bottom Inlet

Fig. 2. (a) shows the distribution tendency at the upper inlet condition. The analysis result shows that the gas fraction tends to be high in channel #2 near the header inlet tube. In contrast, liquid fraction of channel #1 and #4 located at both ends of the header is high and liquid fraction flowing into channel #2 is low. The maximum difference of 3.30%p is observed in the channel #1 when the void fraction is 0.53, and the distribution of CFD follows the experimental results.

The distribution tendency at the bottom inlet conditions is shown in Fig. 2. (b). The analysis result shows that liquid fraction flow into channel #4 at the bottom of the header is high. And liquid fraction liquid fraction

flowing into channel #2, #3 is low due to gas fraction inflow. The liquid fraction shows a maximum difference of 3.85%p at channel #4 when the void fraction is 0.53. Therefore, the bottom inlet case also follows the experimental distribution tendency of liquid phase.

3.2. Effects of inlet position and void fraction

Two-phase flow characteristics according to the void fraction change at each inlet location are analyzed by internal flow. When the two-phase flow develops from the inlet tube, phase separation occurs due to density difference between the liquid phase and the gas phase. As the two-phase flow flows into the header, it collides with the double pipe installed inside the header, and two-phase flow is divided into two branches and flow to the wall of the header. Then the incoming flow creates two vortices. First, since the diameter of the header is larger than that of the inlet tube, vortices and flow separation are generated at the part where the inlet tube and the header are connected. When the flow is passing through the double pipe, like external flow, the second vortices are generated causing separation at the rear end of the double pipe. In the region where the flow separation is generated, the gas phase with small momentum rotates and flows toward the axis direction of header. Fig. 3 shows the cross-sectional contours of volume fraction and velocity vector distribution in the cross-section (yz plane) at the header adjacent to the inlet. In the figure, gas fraction is concentrated in the region close to the inlet tube and in the rear part of the double pipe. As the void fraction increased, the size of the vortex increased.

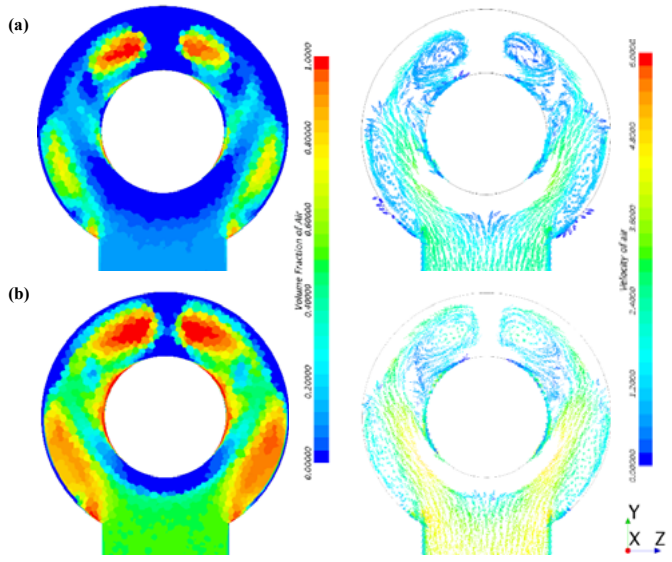

Fig. 3. Cross-Sectional Contours of Void Fraction and Velocity Vector of Header Adjacent to The Inlet: (a) $\alpha = 0.17$, (b) $\alpha = 0.53$

Flow developed at the inlet splits in both directions of the header, while generating a vortex. Volume fraction contours of the header cross-section are shown in Fig. 4.

In the upper inlet case, flows are split two ways that upward direction to channel #1 and downward direction to channel #2, #3, and #4. In each direction, the flow develops while maintaining the vortex and then flows toward the branch tube. Since the liquid phase has a greater momentum than the gas phase, the liquid phase flows toward both ends of the header due to the inertia force. The gas phase tends to flow to the channel located at the center of header. Therefore, the gas phase flowing in the upper part of the inlet cross-section due to phase separation, is directed downward. In the downward section contains channels #2, #3, and #4, due to the momentum difference, the gas phase flows to channels #2 and #3 close to the inlet and the liquid phase flows to channel #4 located at the end of header. The direction of flow and the buoyancy are inconsistent, then the gas phase lose momentum while flowing between channels #2, and #3 and flow back to channels #2.

In the bottom inlet case, the two-phase flow from the inlet generates vortices and develops and is divided into downward direction to channel #4 and the upward direction to channel #1, #2, and #3. The downward

flow to the channel #4 has less gas phase than the upward flow due to the phase separation at the inlet. In addition, because the flow direction is downward, the gas phase flows back to upward due to the buoyancy effect. Therefore, in the case of void fraction 0.17, no gas phase flow to the channel #4, and some gas phase is distributed as the void fraction increased. The upward flow is similar with the downward at upper inlet case. Due to the momentum difference, much of gas phase flow to the channel close to the header. Although little amount of gas phase flows to the channel #4 at the bottom end of header, gas phase flowing upward is distributed more uniform than the upper inlet condition. In order to compare quantitatively to the distribution tendency according to the inlet position, standard deviation of distribution is compared. Table 2 shows the standard deviation of the liquid fraction at upper and bottom inlet case according to the change of void fraction. The distribution tendency of the bottom inlet case is more uniform than the upper inlet case in all void fraction conditions.

Table 2. Standard deviation of liquid fraction according to inlet position

	Upper inlet	Bottom inlet
α=0.17	0.018	0.007
α=0.39	0.050	0.034
α=0.53	0.078	0.067

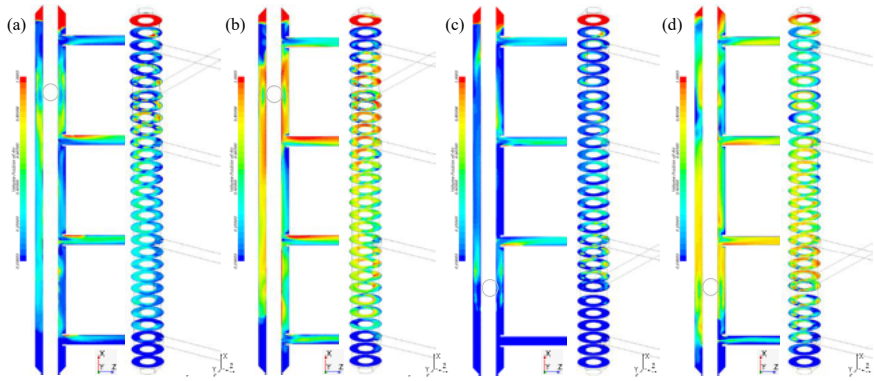

Fig. 4. Contour of Volume Fraction: Upper Inlet (a) $\alpha = 0.17$, (b) $\alpha = 0.53$; Bottom Inlet (c) $\alpha = 0.17$, (d) $\alpha = 0.53$

To compare the velocity of the gas phase and liquid phase and to analyze the change in the magnitude of the momentum in each section, the superficial velocity is compared. The superficial velocity is defined as follows:

$$U_{s,k} = \alpha_k U_k \tag{7}$$

where α_k and U_k represents volume fraction and velocity of the phase k. Fig. 5 is a graph of the axial cross-sectional mean magnitude of superficial velocity inside the header for gas phase and liquid phase at a void fraction of 0.53. The x axis represents the position in the axial direction of the header and the y axis represents the cross-sectional mean superficial velocity. Fig. 5. (a) and (b) are the upper and lower inlet cases, respectively.

The superficial velocity distribution of the liquid phase is the highest at the x=-0.078 m cross-section where the inlet tube is located due to the influence of the mass flow rate from the inlet tube to the header. The liquid flow collides on the rear wall of the header and flows axially in two directions. At the inlet of the header where the liquid flow splits from the wall into bifurcation, creating a vortex, the superficial velocity decreases significantly. As the flow splits in two directions at the inlet of the header, the superficial velocity gradually decreases. Branches are located at the cross-sections at x=0.12 m, 0.04 m, -0.04 m, and -0.12 m, respectively. However, the liquid phase maintains superficial velocity up to channel #1, #4 (x=0.14 m, -0.14 m) at both ends of the header. Comparing the two inlet conditions, the superficial velocity of the liquid phases tended to be the same. But in the bottom inlet case, liquid phase is less distributed to the channel #4 located downwards due to

the influence of gravity. Therefore, the superficial velocity is higher than that of channel #1 in the upper inflow condition.

The gas flow shows different tendency in two cases compared to the liquid phase. Since the phase separation of the gas phase in the inlet tube, most of the gas phase flows in the upper part of the inlet cross-section. In the upper inflow condition, however, most of the gas flowed to downward. Therefore, the highest superficial velocity value is obtained in the cross-section of x=-0.078 m.

However, the bottom inlet case shows the highest superficial velocity at the cross-section of x=-0.07 m rather than x=-0.078 m because the gas phase located at the top of the inlet flows directly to the top of the header. In addition, the upper inlet case is due to the buoyancy, the gas phase flows backward, and most of the flow rate flows into the channel #2. Then the superficial velocity decreases significantly after channel #2 (x=0.04 m). In Fig. 5. (a), the superficial velocity of x=-0.04 m to x=0.04 m is 0.3 m/s. However, the bottom inlet case shows that the superficial velocity decreases relatively uniformly in channels 2 and 3. In Fig. 5. (b), the superficial velocity of the same section is 0.5 m/s, which is relatively high. And in both cases, there is a region filled with gas phase on top of header (x=0.14 m), so the velocity of the liquid phase is zero, but the velocity of the gas phase is not zero.

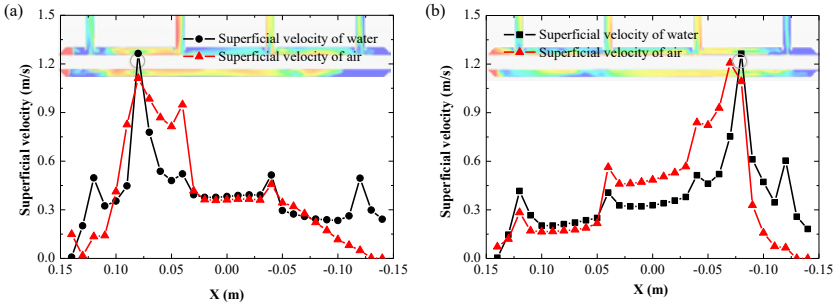

Fig. 5. Cross-Sectional Superficial Velocity Magnitude of Header: (a) Upper Inlet, (b) Bottom Inlet

3.3. Geometry Modification

It is confirmed that uneven distribution occurs when two-phase flow flows into the vertically installed header. Under every condition, most of gas phase flow into the channel #2 and #3, which are close to the header inlet, and most of liquid phase flow into the channel #1 and #4 located at both ends of the header. As the void fraction of the two-phase flow increased, this uneven distribution became more exacerbated.

The factor that most influences the uneven distribution inside the header is the density difference between the two fluids. Due to the difference in the density, phase separation and buoyancy occur, and despite homogeneous flow, the difference in momentum occurs and each phase has a different distribution tendency. The distribution characteristic of two-phase flow is shown in Table 2. The bottom inlet case shows a relatively uniform distribution than upper inlet case because the effect of buoyancy is reduced. Therefore, in this study, the header is modified under the bottom inlet case. In the bottom inlet case, the gas phase mostly flows upward, and the liquid phase is distributed at both ends of the header. To improve distribution, the gas phase flowing through channels # 2 and # 3 must be distributed along with the liquid phase to the end of header. In particular, the # 4 channel has little gas phase due to the buoyancy effect, so it needs to be improved through geometry modification.

Various researchers have tried to improve the distribution by modifying the header design. Webb and Chung [11] attempted to improve the distribution by inserting obstacles such as baffles or weirs inside the header or by inserting inlet tubes. When inserting the obstacle, the incoming two-phase flow created a jet through the obstacle, and each phase were mixed well, then it improved distribution characteristics. However, obstacles depended on the internal geometry of the header. If the part of the geometry changed, the design must be changed accordingly. Mahvi and Garimella [12] and Pistoresi [13] tried to improve the distribution by reducing the cross-section area of the headers instead of inserting obstacles. The header is designed that the cross-section is narrowed from the header inlet to the end, then the mixing of the gas and the liquid phase is improved to have the uniform distribution.

In the case of the header used in this study, since direction of the inlet tube is horizontal and the header is installed vertically and the double pipe is inserted the center of header, the method of reducing the outer diameter of the double pipe header is used. Under the bottom inlet case, it is expected that if the diameter of the header heading toward channel #4 is reduced, the momentum of the gas phase heading to channel #4 is increased, and the liquid fraction of channel #4 is reduced and flow to the upper part of header.

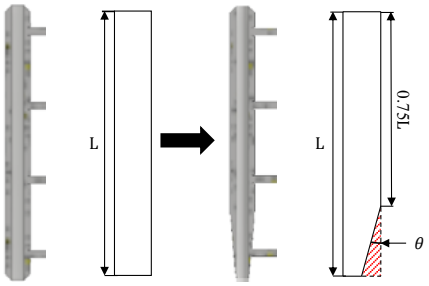

Fig. 6. Schematic of header plane-section modification: (a) Modification Channel #4, (b) Modification Channel #1 and #4

Schematic of the geometry modification of the header is shown in Fig. 6. The diameter of the cross-section from the header inlet to channel #4 is adjusted through the modification angle θ. The modification angle of the header can be converted from 1° to 5°.

The CFD simulation is performed with the void fraction 0.53 condition as a default, which has the largest uneven distribution in the bottom inlet case. The distribution tendency according to the modification angle of the header simulated by CFD is shown in Fig. 7. In the distribution tendency shown in Fig. 7, the distribution is improved as the modification angle increases. Unlike the effect of changing the void fraction, the amount of change in the liquid and gas phases due to the change in modification angle is relatively small. At the bottom of the header, the liquid fraction gradually decreases, but the gas fraction gradually increases. The increasing liquid mass flow rate to the upper side of the header does not change the liquid fraction in channels # 2 and # 3 when the modification angle is changed to 3°. As the angle increases to 5°, the volume fraction change affects to the channel #1, so that the liquid fraction distribution is improved in the upper part of header.

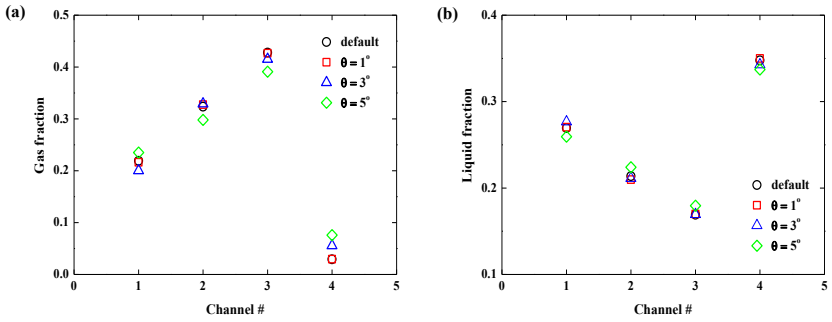

Fig. 7. Effect of header modification angle on flow distribution: (a) Gas Fraction, (b) Liquid Fraction

Table 3. Standard deviation of liquid fraction according to inlet position

Modification angle	Air	Water
Default	0.147	0.067
1°	0.146	0.067
3°	0.136	0.066
5°	0.115	0.058

Table 3 shows standard deviation according to the modification angle. The distribution tendency according to the modification angle is shown through the standard deviation. As the modification angle is increased, the distribution is gradually improved.

4. Conclusion

In this study, the two-phase distribution characteristics of the refrigerant distributor used in the VRF system is investigated by CFD simulation. Internal flow of the header is analyzed by CFD simulation and the factor that affects the uneven distribution of two-phase flow is investigated. The analysis conditions are divided into upper inlet condition and bottom inlet condition according to the header inlet position. For each condition, the flow characteristics in the header are analyzed according to the change of void fraction. Based on the analysis, the geometry of the header is modified to evaluate the two-phase flow distribution characteristics. Some major conclusions are as follows:

- The two-phase flow distribution results simulated by CFD are following the tendency as those measured by the previous experimental study.
- Most of the gas phase flows into the channel close to the inlet tube both the upper inlet and the bottom inlet cases, and the liquid phase flows to the both rear part of the header.
- As the void fraction is increased, uneven distribution is exacerbated.
- When the inlet position is located at the upper part of the header, the buoyancy force acts on the gas phase flowing downward then the gas phase flows counter currently.
- When the inlet is located at the bottom part of the header, a small amount of gas phase is distributed to channel #4, but the overall flow distribution shows less uneven compared to the upper inlet conditions.
- The geometry is modified to narrow the diameter of the headers towards branch 4 to improve the non-uniform distribution.
- As the modification angle is increased, the liquid phase distributed to branch 4 decreases while gas fraction increases.
- Standard deviation results show that the distribution is and improved as the modification angle increased.

References

[1] Dario, E. R., Tadrist, L., Passos, J. C., 2013. Review on two-phase flow distribution in parallel channels with macro and micro hydraulic diameters: Main reults, analyses, tendency. Applied Thermal Engineering. 59, 316-335.
[2] Kim, N. H., Lee, E. J., Byun, H. W., 2012. Two-phase refrigerant distribution in a parallel flow minichannel heat exchanger having horizontal headers. International Joural of Heat and Mass Transfer. 55, 7747-7759.
[3] Vist, S. and Pettersen, J, 2004. Two-Phase Flow Distribution in Compact Heat Exchanger Manifolds. Experimental Thermal and Fluid Science. 28, 209-215.
[4] Lee, J. K. and Lee, S. Y., 2004. Distribution of Two-Phase Annular Flow at Header- Channel Junctions. Experimental Thermal Fluid Science. 28, 217-222.
[5] Zian, J., Ding, M., Bian, H., Zhang, Y., Sun, Z., 2018. CFD simulation for the effect of the header match on the flow distribution in a central-type parallel heat exchanger. Chemical Engineering Research and Design. 136, 144-153.
[6] Said, S. A. M, Ben-Mansour, R., Habib, M. A., Siddiqui, M. U., 2015. Reducing the flow mal-distribution in a heat exchanger. Computer & Fluids. 107, 1-10.
[7] Ham, S. K. and Jeong, J. H., 2018. Two-phase flow distribution according to variation of flow resistance and flow path in manifold shaped distributor. Trans. Korean Soc. Mech. Eng. B, Vol. 2018 No.4, 98~99
[8] Naumann, Z., Schiller, L., 1935. A drag coefficient correlation. Z Ver Deutsch Ing. 77-318.
[9] Shih, T.-H., Zhu, J., Lumbly, J. L., 1995. A new Reynolds stress algebraic equation model. Computor Methods in Applied Mechanics and Engineering. 125, 287-302.
[10] Behzadi, A., Issa, R. I., Rusche, H., 2004. Modelling of dispersed bubble and droplet flow at high phase fractions. Chemical Engineering Science. 59, 759-770.
[11] Webb, R. L., Chung, K, 2005. Two-phase flow distribution to tubes of parallel flow air-cooled heat exchangers. Heat Transfer Engieering. 26, 3-18.
[12] Mahvi, M., Garimella, S., 2017. Visualization of flow distribution in rectangular and triangular header geometries. International Journal of Refrigeration. 76, 170-183.
[13] Pistoresi, C., Fan, Y., Luo, L., 2015. Numerical study on the improvement of flow distribution uniformity among parallel mini-channels. Chemical Engineering and Processing: Process Intensification. 95, 63-71.